World Journal of Innovative Research (WJIR)
ISSN: 2454-8236, Volume-14, Issue-3, March 2023 Pages 01-08

Cross-plot Analysis of Rock Physics attributes in the G–Field onshore Niger Delta Basin

Balogun Ayomide Olumide, Oguka Valentina Omojevwe

***Abstract*— Cross-plot analyses of rock physics attributes were carried out to evaluate hydrocarbon charged reservoir in G–Field onshore Niger Delta Basin in other to reduce the ambiguity and risk associated with fluid and lithology discrimination using well logs. The well based rock physics attribute cross-plots used were Lambda-Rho against Mu-Rho, Lambda-Rho against Vp/Vs ratio, Lambda-Rho against P-Impedance and Vp/Vs ratio against P-Impedance colour-coded with various reservoir properties such as gamma ray, density, resistivity, and water saturation to successfully distinguish between fluids and lithology. The results showed that Hydrocarbon-saturated sand, shale, and brine sand zones were distinguished in the reservoir using cross-plots of P–Impedance, Lambda-Rho, Mu-Rho, and V_P/V_S ratio. The results from well-based cross plot analysis showed that hydrocarbon sands have low P–Impedance, V_P/V_S, Lambda-Rho and Mu-Rho values. P–Impedance and V_P/V_S are sensitive to both fluid and lithology whereas Lambda-Rho is only sensitive to fluid and Mu-Rho is only sensitive to rock matrix. The low values observed for hydrocarbon sands as relative to shale, are defining trait of Niger Delta fields that originates from the reservoir's unconsolidated nature.**

***Index Terms*—Rock physics attribute, Cross-plot analysis, Property attribute, Fluid and lithology**

I. Introduction

The Niger Delta is a major hydrocarbon zone in the world. The basin having prominent geological features and conserved thick sedimentary deposits are highly favorable for petroleum generation, migration, and confinement from onshore through the continental shelf and deep-water terrains. It is notable as one of the major productive deltaic oil and gas accumulation, been the largest basin in the West African continental margin [1]. The Agbada Formation, which contains numerous vertically stacked reservoir structures, traps hydrocarbons primarily in sandstones and unconsolidated sands. However, the traps and structures constitute a significant challenge in mapping due to their complexities, majorly in structural distortions [2]. The identification and delineation of reservoir lithology also shape part of the major challenges faced by exploration geoscientists during field planning, appraisal, and drilling owing to the heterogeneous nature of the subsurface. Therefore integration of different datasets for accurately building reservoir models is essential for the characterization of these reservoirs [3].

Balogun Ayomide Olumide, Department of Physicse, University/ of Port Harcourt, Choba, Rivers State, Nigeria
Oguka Valentina Omojevwe, Department of Physicse, University/ of Port Harcourt, Choba, Rivers State, Nigeria

Delineating a reservoir in adequate detail is a prerequisite in the appraisal stage of the development cycle of every hydrocarbon field. This stage precedes the development of a field for commercial production and helps ascertain the field's economic potential. The absence of a comprehensive and robust report of reservoir characterization study has affected the development of the field such that optimum recovery rate has not been achieved, since uncertainties in well placement has not been effectively minimized. Hence this research in the study area will help to make appropriate decisions on development, production, and completion.

II. LOCATION OF THE STUDY AREA

The study area is an oil field located within the onshore, southwestern part of the coastal swamp depobelt region of the Niger Delta, within latitude 3°N and 6°N and longitude 5°E and 8°E (Fig.1). For the purpose of this work this field will be designated as G–Field.

Fig 1: Location of G–field (study area highlighted by the blue-hashed square in Niger Delta [4].

The Niger Delta is made up of an overall regressive clastic sequence, covering area of approximately 75,000 Km^2 with an average thickness of about 12 Km and it is located in the southern part of Nigeria, West African in the Gulf of Guinea [5], [6]. The Niger Delta resulted from the separation of the African and South American plates starting in the Late Jurassic and continuing into the Cretaceous [7]. It is a major hydrocarbon province in the world. The Niger Delta has one identified petroleum system known as the Tertiary Niger Delta (Akata-Agbada) petroleum system [5], [6], [7], [8], [9],

[10]. Three lithostratigraphy (Akata, Agbada and Benin Formations) are present in the basin [11].

The main source rock made up of shale is the Akata Formation while the Agbada Formation made up of alternation of sand and shale is the main reservoir lying on top of the Akata Formation. Lying on the Agbada Formation is the Benin Formation made up of sand lithology [7].

Fig. 2 shows the base map of the seismic field. The data were acquired from G-field located in onshore Niger-Delta.

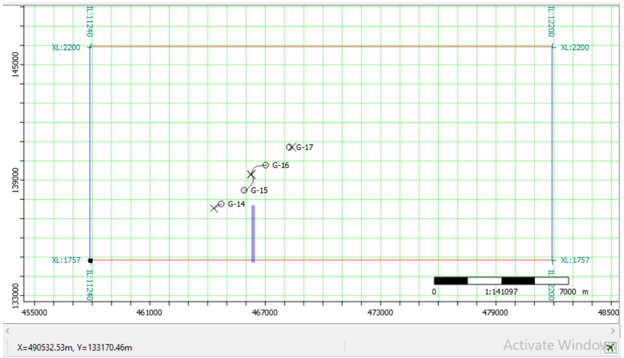

Fig. 2: Base Map of the study area.

A. *Theoretical Backgrounds*

Lame's Lambda constant (λ)

The measure of the fluid's ability to resist compression, hence it is sensitive to pore fluid and sometimes called fluid incompressibility. It relates with bulk modulus (K) according to the expression;

$$\lambda = K - \frac{2\mu}{3} \qquad 1$$

Lambda-Mu-Rho $(\lambda - \mu - \rho)$

Lambda-Mu-Rho attributes was first introduced by [12], where Mu-Rho was defined as the multiplication of rock density and rigidity and expressed as;

$$V_P = \sqrt{\frac{\lambda + 2\mu}{\rho}} \qquad 2$$

$$V_S = \sqrt{\frac{\mu}{\rho}} \qquad 3$$

Therefore, $I_S^2 = (\rho V_S)^2 = \mu\rho$

$$\mu\rho = I_S^2 \qquad 4$$

whereas the μ term or rigidity, is sensitive to rock matrix and Lambda-Rho $(\lambda\rho)$ defined as;

$$I_P^2 = (\rho V_P)^2 = (\lambda + 2\mu)\rho$$

$$\lambda\rho = I_P^2 - 2I_S^2 \qquad 5$$

$$\lambda\rho = I_P^2 - c\,I_S^2$$

Where c is the discriminator factor ranging from "2 to 2.233" for robust discrimination of fluid and lithology [13], "I_S" and "I_P" are S-wave and P-wave Impedances, respectively.

III. Materials and Methods

The data set for this work include a suite of well logs consisting of gamma ray (GR), true resistivity (RT), bulk density (RHOB), neutron porosity (NPHI), compressional sonic (DT), caliper (CALI), Spontaneous Potential (SP) and checkshot (CS) obtained from four deviated wells; G-14, G-15, G-16 and G-17 (Table 1). The composite logs are shown in Figs. 3 – 6. Hampson Russell (HR) software suite was used for the data processing, well log data loading and the cross-plot analysis. To generate the rock physics attribute S-wave velocity was first derived using the empirical formula given by Castagna's mud rock line equation

$$V_P = 1.16V_S + 1360ms^{-1} \qquad 6$$

Thereafter, P–impedance, S–Impedance, V_P/V_S ratio, rigidity modulus (μρ) and Incompressibility modulus (λρ) were transformed from existing P-wave velocity, derived S-wave velocity, and density logs. Cross-plots were then carried out for the discrimination of fluid and lithology using the well logs data.

Table 1: Suite of Logs in each Well.**(Y=YES, N=NO)**

WELLS	**AVAILABLE LOGS**							
	GR	RT	RHOB	NPHI	DT	CALI	SP	CS
G-14	Y	Y	Y	Y	Y	Y	Y	Y
G-15	Y	Y	Y	Y	Y	Y	Y	Y
G-16	Y	Y	Y	Y	Y	N	Y	Y
G-17	Y	Y	Y	Y	N	N	N	N

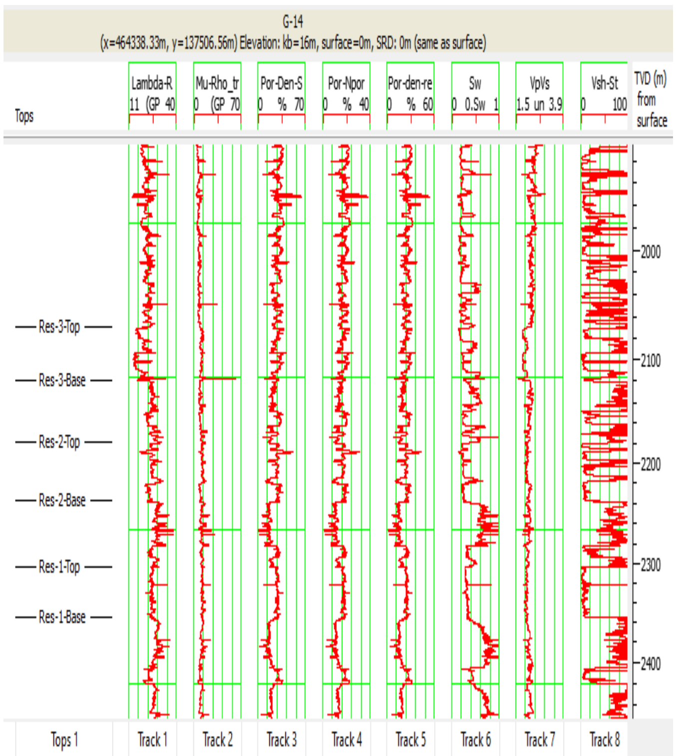

Fig. 3: Petrophysical logs for the three reservoirs intervals for G-14.

World Journal of Innovative Research (WJIR)
ISSN: 2454-8236, Volume-14, Issue-3, March 2023 Pages 01-08

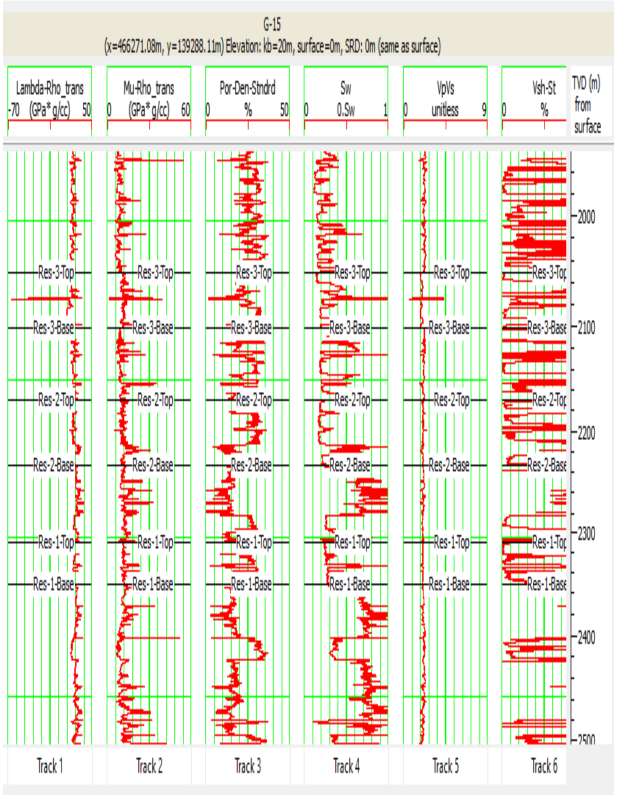

Fig. 4: Petrophysical logs for the three reservoirs intervals for G-15

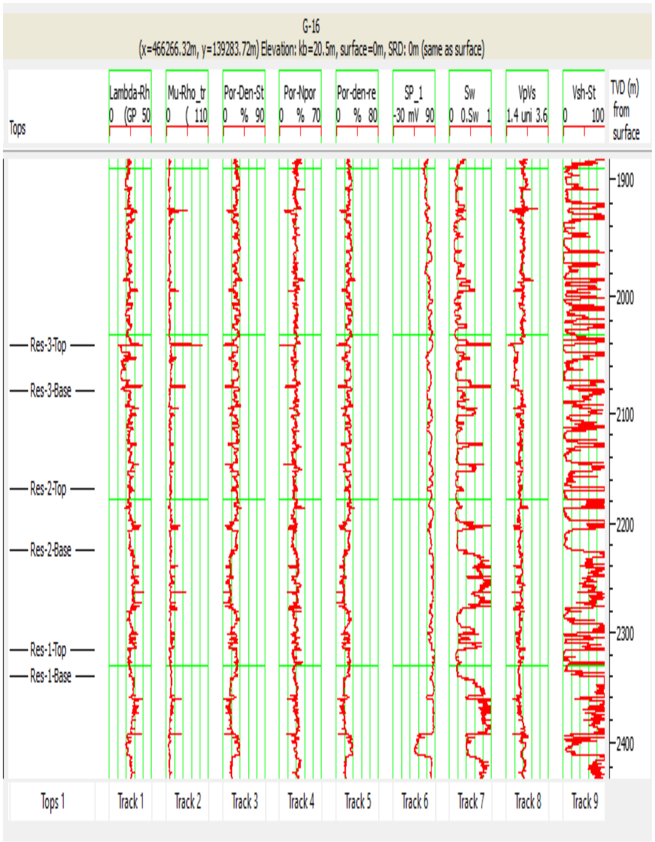

Fig. 5: Petrophysical logs for the three reservoirs intervals for G-16

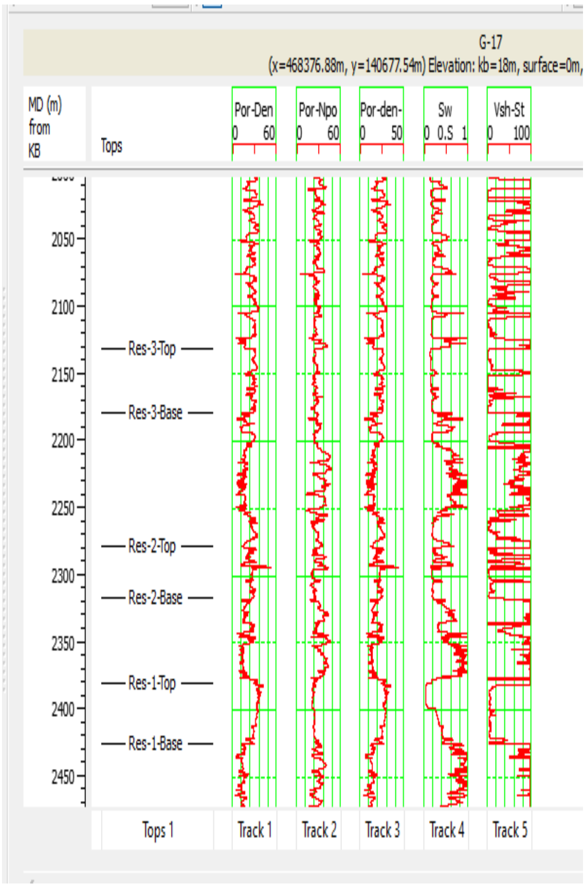

Fig. 6: Petrophysical logs for the three reservoirs intervals for G-17.

IV. RESULTS AND DISCUSSION

Cross-plots are graphical representations of the correlation between two or more independent variables that are used to visually identify anomalies that could be interpreted as the existence of hydrocarbons or other fluids and lithologies [14]. In this study, the cross-plots of the following were carried out;

1. Lambda-Rho against Mu-Rho
2. Lambda-Rho against V_P/V_S ratio
3. Lambda-Rho against P-Impedance and
4. V_P/V_S ratio versus P-Impedance

They were colour-coded with various reservoir properties such as gamma ray, density, resistivity, and water saturation to successfully distinguish between fluids and lithology. The reservoir properties were found to have a linear relationship. The observed results correspond with findings made by [15]. Resistivity log was used to colour-code the cross-plotted area to give an indication of the presence of hydrocarbon within the cross-plotted depth interval. A very high value of resistivity is an indication of the presence of a less conductive fluid than brine. Such high resistivity values are an indication of the presence of a more resistive media such as hydrocarbon, which could be partially or completely replacing brine in the reservoir.

A. Lambda-Rho (λρ) versus Mu-Rho (λρ)

According to [12], Lambda-Rho (λρ) is a pore-fluid indicator, and λρ is an excellent geomorphic indicator. At Reservoir 3, a cross-plot of these two attributes were established for lithology and fluid discrimination (Figs. 7 – 10). Three cluster zones were defined that correspond to Shale (purple sphere), Brine (Blue sphere) and Hydrocarbon sand (red sphere) lithology. Both attributes were capable of distinguishing the lithology types. A low Gamma ray colour-code validated the defined geological structures, with the least value concentrated in the sand geomorphic cluster and the highest values concentrated in the shale (Fig. 7). The resistivity colour-codes on the points affirmed that the zone with the lowest Lambda-Rho values has the highest resistivity feedback, indicating that the zone is hydrocarbon-bearing (Fig. 8). High lambda-rho values, as found in brine sand and shale lithology, indicate greater incompressibility, according to [16]. Shale lithology has lower Mu-Rho values than sand and can be used to distinguish between the two. A careful examination of the cross-plot (Fig. 9) reveals that clusters with the least water saturation correspond to high resistivity, which implies highly charged hydrocarbon saturation sand.

Similarly, clusters with maximum water saturation correspond to the lowest resistivity value. This shows the conducting potential of interstitial water, and hydrocarbon opposition to the flow of current. The zone with the lowest Lambda-Rho and Mu-Rho values has the lowest density colour code, indicating that the zone is hydrocarbon bearing sand and relatively higher Lambda-Rho, Mu-Rho and density values is associated with shale/brine-sand within the reservoir (Fig. 10). The hydrocarbon-bearing zone was excellently separated by the brine filled sand, as seen in the cross-plot, indicating its sensitivity to fluid change. Low Lambda-Rho values with little variation in Mu-Rho are indicators of the presence of hydrocarbon sand [17], [18]. The cross-plots therefore, show a good result for both lithology and fluid discrimination.

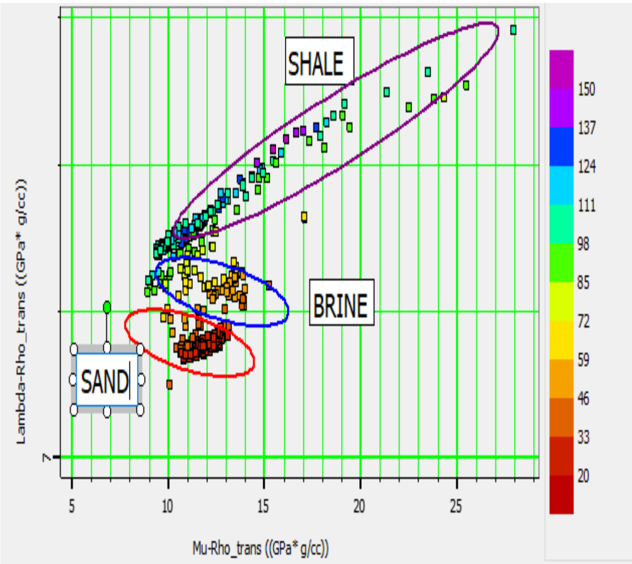

Fig. 7: Cross-plot of Lambda-Rho (λρ) versus Mu-Rho (λρ) versus colour-coded with Gamma ray.

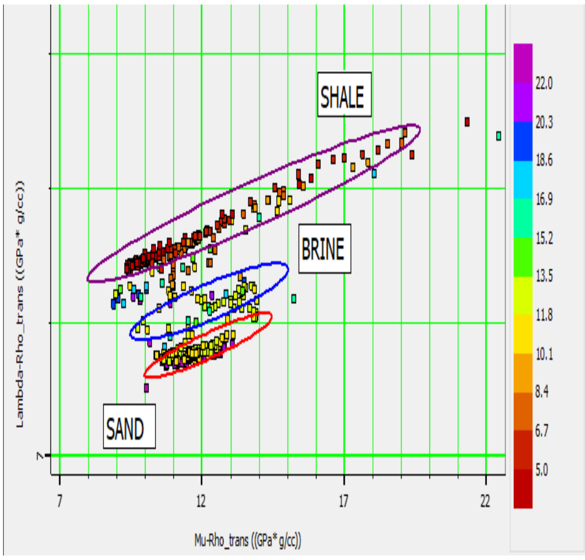

Fig. 8: Cross-plot of Lambda-Rho (λρ) versus Mu-Rho (λρ) versus colour-coded Resistivity.

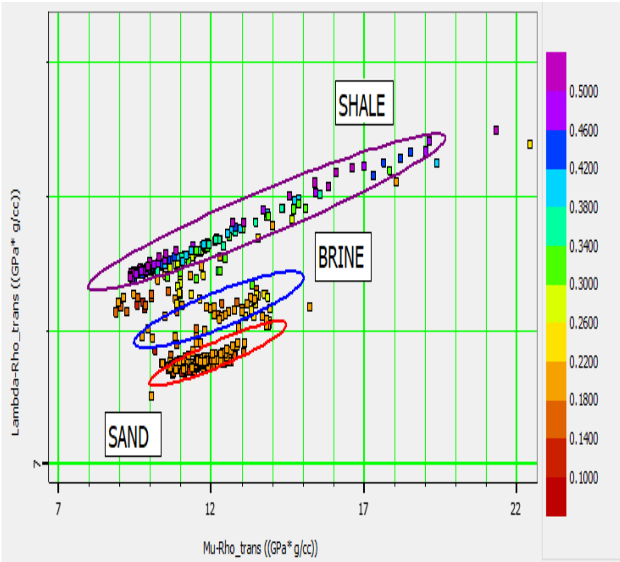

Fig. 9: Cross-plot of Lambda-Rho (λρ) versus Mu-Rho (λρ) versus colour-coded with Water Saturation

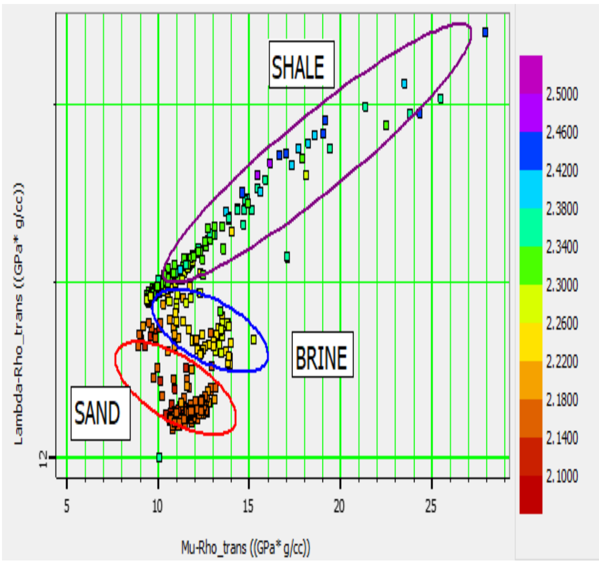

Fig. 10: Cross-plot of Lambda-Rho (λρ) versus Mu-Rho (λρ) versus colour-coded with Density

B. Lambda-Rho (λρ) versus V_P/V_S ratio

Hydrocarbon sand zone (red sphere) is marked by with low values in both V_P/V_S ratio and Lambda-Rho. This cross-plot distinguishes between fluid and lithology (Figs. 11 – 14). The hydrocarbon sand zone exhibits good reservoir quality, as evidenced by low water saturation values (Fig. 13) and the presence of hydrocarbon marked by high resistivity value clusters (Fig. 12). The shale zone (purple sphere) is defined by the high gamma ray and low resistivity value (Fig. 11). The zone with the lowest Lambda-Rho and V_P/V_S values has the lowest density colour code, indicating that the zone is hydrocarbon-bearing sand and relatively higher lambda-Rho, V_P/V_S and density values is associated with shale/brine-sand within the reservoir (Fig. 14).

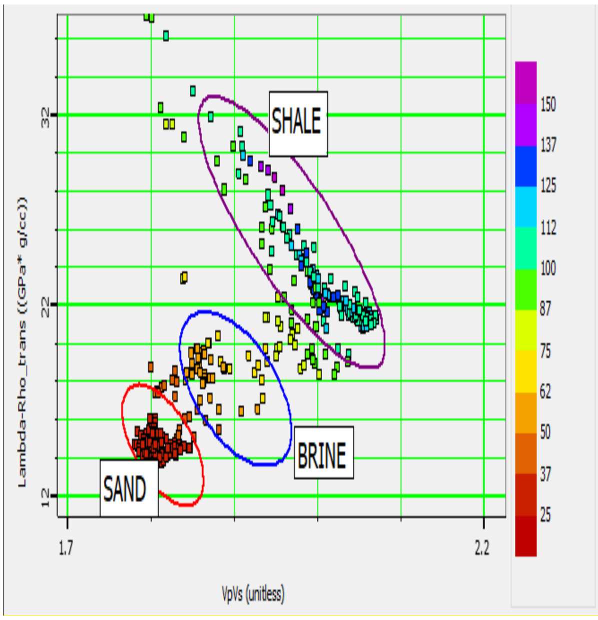

Fig. 11: Cross-plot of Lambda-Rho (λρ) versus V_P/V_S Ratio colour-coded with Gamma ray

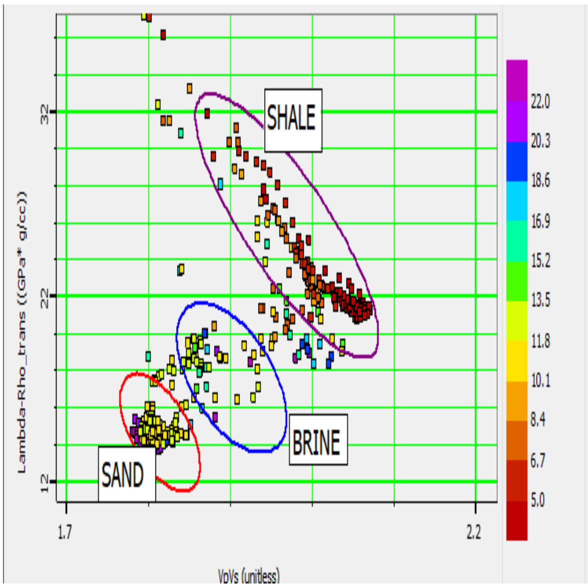

Fig. 12: Cross-plot of Lambda-Rho (λρ) versus V_P/V_S Ratio colour-coded with Resistivity.

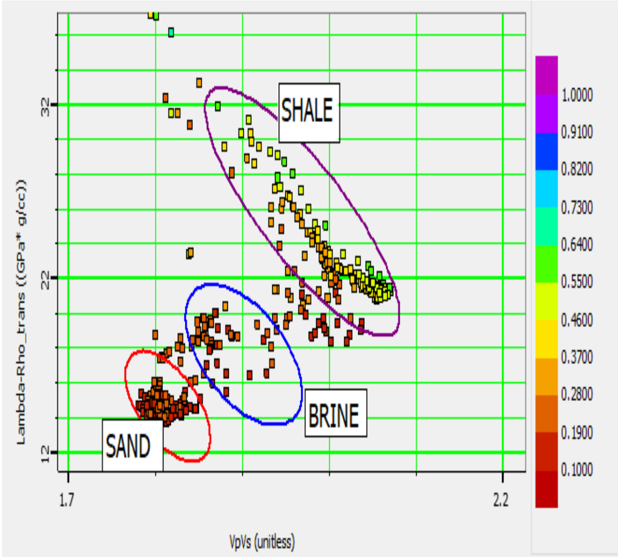

Fig. 13: Cross-plot of Lambda-Rho (λρ) versus V_P/V_S Ratio, colour-coded with Water Saturation.

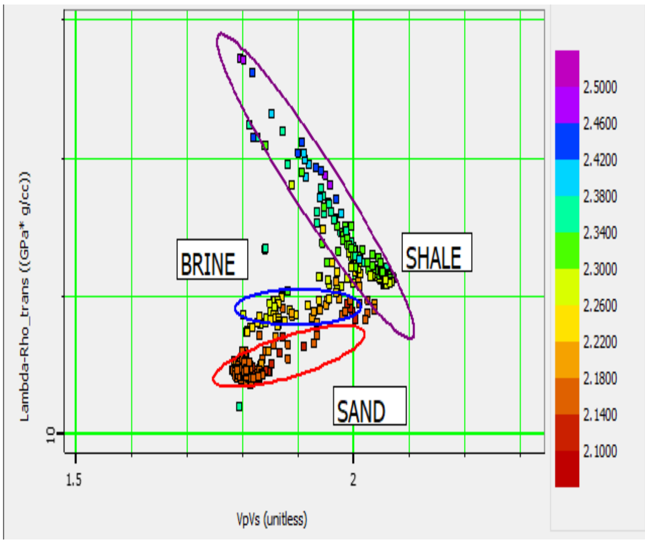

Fig. 14: Cross-plot of Lambda-Rho (λρ) versus V_P/V_S Ratio colour-coded with Density

C. Lambda-Rho (λρ) versus P-Impedance

The cross-plot clearly distinguishes between hydrocarbon-bearing sands (red sphere) and shale (purple sphere). In the plot, the lowest values of Lambda-Rho and P–Impedance associated with hydrocarbon are validated as sands lithology (Figs 15 – 18). In terms of fluid content, both Lambda-Rho and P–Impedance show good discrimination, according to the plot. This is because high and low P–Impedance indicates shale and sand, respectively, while decreasing Lambda-Rho values clearly identify the different fluid types in the sand lithology, from brine to gas. A better reservoir is said to have lower P–Impedance values with lower density and velocity (Fig. 18). The plot also showed the gamma ray colour-code affirming that the zone with the lowest Lambda-Rho and P–Impedance values has the lowest gamma ray (Fig. 15) and water saturation (Fig. 17) with highest resistivity (Fig. 16) feedbacks, indicating that the zone is hydrocarbon bearing sand.

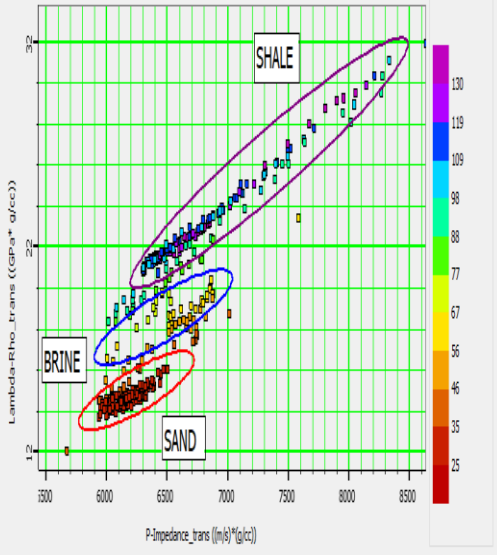

Fig. 15: Cross-plot of Lambda-Rho(λρ) versus P-Impedance colour-coded with Gamma ray

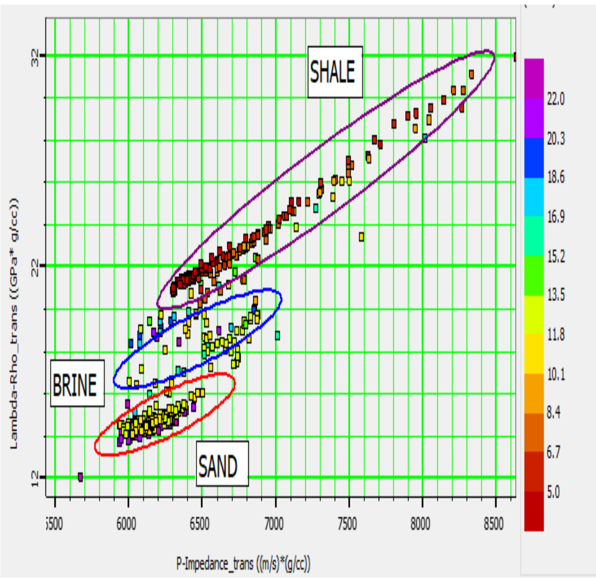

Fig. 16: Cross-plot of Lambda-Rho(λρ) versus P-Impedance colour-coded with Resistivity

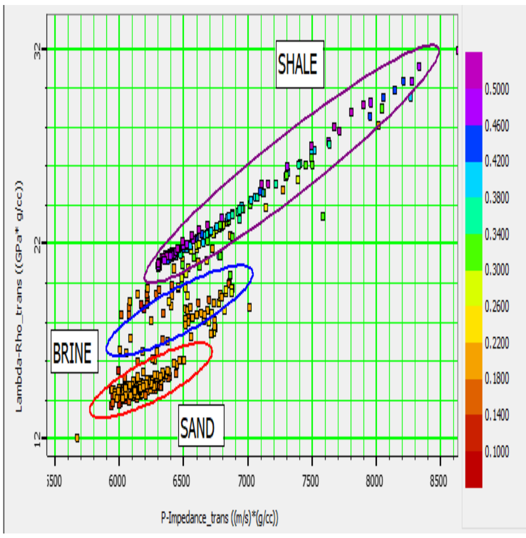

Fig. 17: Cross-plot of Lambda-Rho(λρ) versus P-Impedance colour-coded with Water Saturation.

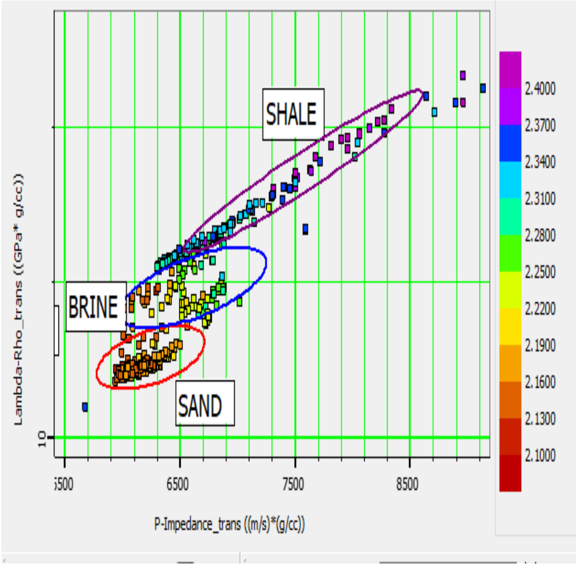

Fig. 18: Cross-plot of Lambda-Rho(λρ) versus P-Impedance colour-coded with Density

D. V_P/V_S ratio versus P–Impedance

The cross-plot successfully discriminated the reservoir into three zones; hydrocarbon sand (Low value in both attributes, identified using red sphere), brine (blue sphere) and shale (High value in both attributes, identified using the purple sphere) (Figs. 19 – 22). The Gamma ray colour-code affirms the defined lithology by showing high gamma ray values for the shale zone and a lower value for the sand zone (Fig. 19). The V_P/V_S vs P–Impedance ratio is a good fluid-lithology indicator as low V_P/V_S ratio indicates a clean sand lithology which may be hydrocarbon saturated which show low water ssaturation (Fig. 21) and high resistivity (Fig. 20) while a higher V_P/V_S ratio indicates shale lithology [19], [20]. P–Impedance values are higher in shale due to greater compaction feedback, but lower in sand and significantly lower in hydrocarbon-bearing sands. The cross-plots depict data point clusters, with each cluster defined by a coloured sphere differentiating the hydrocarbon-bearing zone from the brine sand and shale zones.

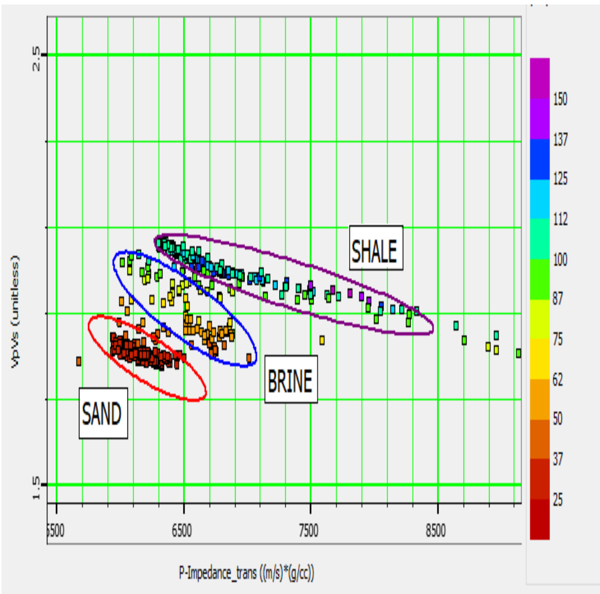

Fig 19: Cross-plot of V_P/V_S Ratio versus P-Impedance colour-coded with Gamma ray

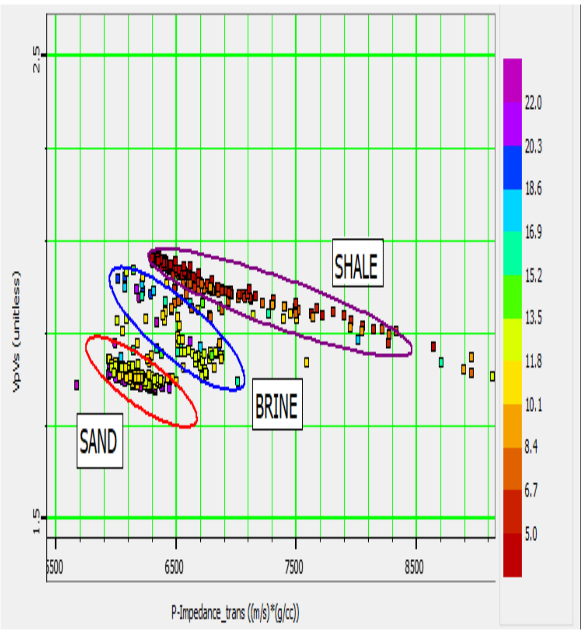

Fig. 20: Cross-plot of V_P/V_S Ratio versus P-Impedance colour-coded with Resistivity

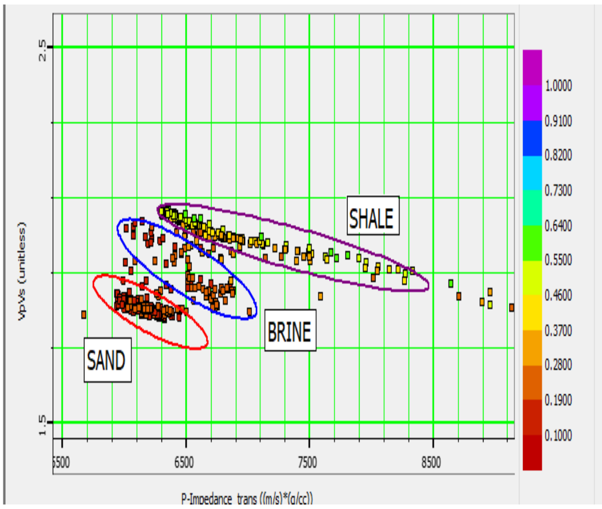

Fig. 21: Cross-plot of V_P/V_S Ratio versus P-Impedance colour-coded with Water Saturation.

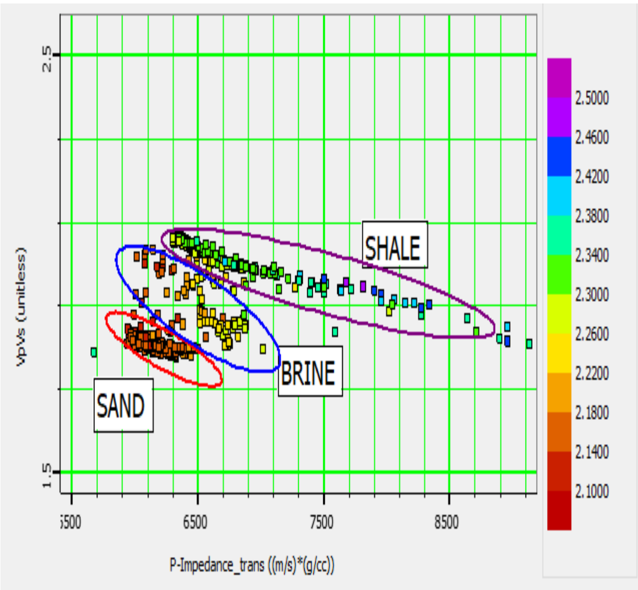

Fig. 22: Cross-plot of V_P/V_S Ratio versus P-Impedance colour-coded with Density

Well development and exploration has high prospects in regions with low P–Impedance (indicating high reservoir porosity) and corresponding low V_P/V_S ratio (indicating hydrocarbon accumulation). The P–Impedance of the reservoir sand medium is usually lower than that of the surrounding shale formation in hydrocarbon-saturated reservoir (Figs. 19 – 22). The relatively higher V_P/V_S, P–Impedance and density (colour-code) value is associated with shale/brine-sand within the reservoir (Fig. 22) [16]. This underlines the fact that velocity and density are proportional in a rock formation, and also validates Gardner's relation.

V. Conclusion

Hydrocarbon-saturated sand, shale, and brine sand zones were distinguished in the reservoir using cross-plots of P–Impedance, Lambda-Rho, Mu-Rho, and V_P/V_S ratio. These well cross-plots show that hydrocarbon sands have low P–Impedance, V_P/V_S, Lambda-Rho and Mu-Rho values. P–Impedance is sensitive to both fluid and lithology whereas Lambda rho is only sensitive to fluid and Mu-rho is only sensitive to rock matrix. A low P–Impedance value indicates hydrocarbon-bearing sands while high P–Impedance zones indicate shale/flooding zones. Lower P-wave velocity is observed in reservoir rock containing fluids that is oil and gas that is compressible, by implication hydrocarbon-bearing sands will have a lower P–Impedance value than water bearing sands. Vp/Vs ratio shows low values for hydrocarbon reservoir sands and high for non-reservoir sands and this is indictive of lithology discrimination [21], [22]. This is because the sensitivity of P-wave velocity is more in fluid changes than the S-wave velocity, when fluid content changes it will result in changes in Vp/Vs. Here, it is observed that Vp/Vs, ratio for hydrocarbons is generally lower than shale/brine sand. Mu-Rho shows medium to high values indicating sand and low for shale, this attribute in turn is indicative of lithology. The zone with the lowest Lambda-Rho and density values, indicate hydrocarbon saturated sand and relatively higher lambda-Rho and density values is associated with brine-sand /shale within the reservoir, these attributes in turn are indicative of the pore fluid. The low values observed for hydrocarbon sands as relative to shale, are defining traits of Niger delta fields that originates from the reservoir's unconsolidated nature.

Acknowledgment

We acknowledge the assistance of Shell Petroleum Development Company for graciously releasing the data to us for this study. We wholeheartedly acknowledge Late Engr. Enajero Joesph Oguka and Mrs. Augustina Oguka who have been the source of support, inspiration and strength.

References

[1] G. Emujakporue, C. Nwankwo, and L. Nwosu. integration of well logs data and seismic data for prospects evaluation of an X Field, onshore Niger Delta, *Nigeria. International Journal of Geosciences*, 3(4A), 2012, 872-877.

[2] A. P. I. Aizebeokhai and I. Olayinka. Structural and stratigraphic mapping of Emi Field, offshore Niger Delta. *Journal of Geology and Mining Research*. 3(2), 2011, 25-38.

[3] O. Chidi. 3d Seismic Interpretation and Reservoir Characterization of “Diba Field’’, Niger Delta, Nigeria. *Afribary*. 2021. Retrieved from https://afribary.com/works/3d-seismic-interpretation-and-reservoir-characterization-of-diba-field-niger-delta-nigeria-1

[4] O. Agbasi, S. Sen, N. Inyang, and S. Etuk. Assessment of pore pressure, wellbore failure and reservoir stability in the Gabo field, Niger Delta, Nigeria -Implications for drilling and reservoir management. *Journal of African Earth Sciences*, 2020, 173. 104038.

[5] K. Burke, T. F. Dessauvagie and A. J. Whiteman. The opening of the Gulf of Guinea and the geological history of the Benue Trough and the Niger Delta. *Nature* 233, 1971, 51–55

[6] C. M. Ekweozor and E. M. Daukoru. Petroleum source bed evaluation of Tertiary Niger-Delta. *American Association of Petroleum Geologists, Bulletin*, 70, 1984, 48–55

[7] G. O. Emujakporue and E. E. Enifome. Identification of seismic attributes for hydrocarbon prospecting of Akos field, Niger Delta, Nigeria. *SN Applied Sciences*, 2, 2020, 910 |https://doi.org/10.1007/s42452-020-2570-1

[8] J. M. Orife and A. Avbovbo. Stratigraphic and unconformity traps in the Niger Delta, *American Association of Petroleum Geologists, Bulletin*, 65, 1982, 251–265

[9] T. J. A. Reijer. Selected chapters on geology, sedimentary geology, sequence stratigraphy: Three case studies: A field guide. SPDC corporate reprographic service, Warri, Nigeria, 194, 1996

[10] M. L. W. Turtle, R. R. Charpentier and M. E. Brownfield. The Niger Delta Petroleum System: Niger Delta Province, Nigeria, Cameroun, and Equatorial Guinea, Africa. U.S.G.S. Open file Report, 1999, 50 – 54.

[11] B. D. Evamy, J. Haremboure, P. Knaap, F. A. Molloy and P. H. Rowlands. Hydrocarbon habitat of tertiary Niger Delta. *American association of petroleum geologist. Bulletin*, 62, 1978, 1–39

[12] B. Goodway, T. Chen and J. Downton. Improved AVO Fluid Detection and Lithology Discrimination using Lame Petrophysical Parameters fluid stack from P and S –inversion. *CSEG*, 1997, 148-151.

[13] L. M. Omudu, J. O. Ebeniro, N. Osayande and S. Adesanya. Lithology and fluid discrimination from elastic rock properties cross plot: Case study from Niger Delta. Proceeding, 24th Annual, International Conference and Exhibition of Petroleum Explorationist (NAPE) Abuja, Nigeria. 2006.

[14] L. M. Omudu, J. O. Ebeniro and S. Olotu. Optimizing quantitative interpretation for reservoir characterization: case study onshore Niger Delta. In: A paper presented at the 31st annual SPE international technical conference and exhibition in Abuja, Nigeria, 2007, 1-55.

[15] A. Alabi and P. A. Enikanselu. Integrating seismic acoustic impedance inversion and attributes for reservoir analysis over ‘DJ’ Field, Niger Delta. *J Petrol Explor Prod Technol*, 9(4), 2019, 2487–2496.

[16] L. M. Omudu, J. O. Ebeniro. Cross plotting of rock properties for fluid discrimination using well data in offshore Niger Delta. *Nig. J. Physics*, 17, 2005, 16-20.

[17] M. Burianyk. Amplitude-versus-offset and seismic rock property analysis: A primer. *CSEG Recorder*, 25(9), 2000, 6–16.

[18] J. Dewar. Rock physics for the rest of us - An informal discussion. The *Canadian Society of Exploration Geophysicist Recorder*, 5, 2001, 43 – 49.

[19] S. Assefa, C. McCan and J. Sothcott. Velocity of compressional and Shear waves in Limestone. *Geophysical Prospecting*, 51(1), 2003, 1-15.

[20] J. O. Ebeniro, R. S. Dike, L. O. Udochu and A. A. Ezebilo. Cross plotting and hydrocarbon indication in the Niger Delta. NAPE international conference and exhibitions, Abuja, Nigeria. 2003

[21] G. Pickett. Acoustic Character Logs and their applications in formation evaluation. *J. Petr. Tech*, 1963, 659 – 667.

[22] J. P. Castagna, M. L. Batzle, and R. L Eastwood. Relationships between compressional-wave and shear-wave velocities in clastic silicate rocks: *Geophysics*, 50(4), 1985, 571-581.